The soil microbiome of shiro reveals the symbiotic relationship between Tricholoma bakamatsutake and Quercus mongolica

Hongbo Guo[1, 2], Liu WeiYe[3], Yuqi Xie[1], Zhenyu Wang[1], Chentong Huang[1], Jingfang Yi[3], Zhaoqian Yang[3], Jiachen Zhao[3], Lidiya A. Sibirina[2, 4*], Xiaodan Yu[3*]

[1]College of Life Engineering, Shenyang Institute of Technology, China, [2]Primorskaya State Academy of Agriculture, Russia, [3]Shenyang Agricultural University, China, [4]Federal Scientific Center of the East Asia Terrestrial Biodiversity, Far Eastern Branch of the Russian Academy of Sciences, Russia

Submitted to Journal:
Frontiers in Microbiology

Specialty Section:
Microbial Symbioses

Article type:
Original Research Article

Manuscript ID:
1361117

Received on:
25 Dec 2023

Journal website link:
www.frontiersin.org

Scope Statement

Tricholoma bakamatsutake is an edible ectomycorrhizal fungus with increasing demand; however, its cultivation has yet to be achieved. In order to better understand its natural symbiotic relationships, we investigated Quercus mongolica and T. bakamatsutake-associated bacteria and the physicochemical properties and microbiome of the rhizosphere. We collected T. bakamatsutake root rhizosphere (Tb group) and corresponding environmental soil (CK group) samples from different areas and analyzed them for their physicochemical properties and microbiome structure. The results showed that T. bakamatsutake not only directly provided water and minerals to Q. mongolica, but also promoted the growth of the host by regulating the soil microbial community structure. This study is important for constructing a healthy soil microbial community structure and cultivating T. bakamatsutake-Q. mongolica mycorrhizal seedlings.

Conflict of interest statement

The authors declare that the research was conducted in the absence of any commercial or financial relationships that could be construed as a potential conflict of interest

CRediT Author Statement

Zhaoqian Yang: Investigation, Resources, Writing – original draft. Zhenyu Wang: Investigation, Resources, Writing – original draft. Chentong Huang: Investigation, Resources, Writing – original draft. Yuqi Xie: Investigation, Resources, Writing – original draft. Jingfang Yi: Resources, Validation, Writing – original draft. Hongbo Guo: Conceptualization, Data curation, Formal Analysis, Funding acquisition, Project administration, Supervision, Validation, Writing – original draft, Writing – review & editing. Jiachen Zhao: Software, Visualization, Writing – original draft. Lidiya Alekseevna Sibirina: Conceptualization, Methodology, Project administration, Supervision, Validation, Writing – original draft, Writing – review & editing. Liu WeiYe: Data curation, Formal Analysis, Investigation, Methodology, Software, Visualization, Writing – original draft, Writing – review & editing. Xiaodan Yu: Conceptualization, Data curation, Formal Analysis, Funding acquisition, Project administration, Resources, Supervision, Validation, Writing – original draft, Writing – review & editing.

Keywords

shiro soil, ectomycorrhizal fungi, Quercus mongolica, Rhizosphere microorganisms, Symbiotic system, Tricholoma bakamatsutake

Abstract

Word count: 187

Tricholoma bakamatsutake is a delicious and nutritious ectomycorrhizal fungus. However, its cultivation is hindered owing to limited studies on its symbiotic relationships. Hence, we aimed to investigate its symbiotic relationships with Quercus mongolica-T. bakamatsutake-associated bacteria and the physicochemical properties and microbiome of its rhizosphere. In this study, T. bakamatsutake shiro soil (Tb group) and corresponding Q. mongolica rhizosphere soil (CK group) samples were collected from different areas and analyzed for their physicochemical properties and microbiome structure. The Tb group samples had significantly higher sand content and lower levels of total and available phosphorus than those in the CK group soil samples. The microbiome analysis revealed that T. bakamatsutake within the symbiotic system had a significant dominant effect, altering its shiro microbiome structure by suppressing other microorganisms, such as Russula, another ectomycorrhizal fungus, and Penicillum, a phytopathogenic bacteria. The accompanying bacteria, including mycorrhizal-helper bacteria and plant growth-promoting bacteria, were aggregated. Moreover, the microbiome in the symbiotic system was significantly involved in the catabolism of sugars and fats. Our findings elucidated the microbial community and relevant symbiotic environment to further understand the relationship between T. bakamatsutake and Q. mongolica.

Funding information

This study was supported by Science and Technology Plan Project of Liaoning Province (2022-MS-418) and the National Natural Science Foundation of China (32370008).

Funding statement

The author(s) declare financial support was received for the research, authorship, and/or publication of this article.

Ethics statements

Studies involving animal subjects
Generated Statement: No animal studies are presented in this manuscript.

Studies involving human subjects
Generated Statement: No human studies are presented in the manuscript.

Inclusion of identifiable human data
Generated Statement: No potentially identifiable images or data are presented in this study.

Data availability statement

Generated Statement: The datasets presented in this study can be found in online repositories. The names of the repository/repositories and accession number(s) can be found in the article/supplementary material.

The soil microbiome of shiro reveals the symbiotic relationship between *Tricholoma bakamatsutake* and *Quercus mongolica*

Hongbo Guo[1,3#], Weiye Liu[2#], Yuqi Xie[1], Zhenyu Wang[1], Chentong Huang[1], Jingfang Yi[2], Zhaoqian Yang[2], Jiachen Zhao[2], Xiaodan Yu[2]*, Lidiya Alekseevna Sibirina[3,4]*

[1] *College of Life Engineering, Shenyang Institute of Technology, Fushun 113122, China*

[2] *College of Biological Science and Technology, Shenyang Agricultural University, Shenyang 110866, China*

[3] *Primorye State Agricultural Academy, Ussuriisk 692525, Russia*

[4] *Federal Scientific Center of the East Asia Terrestrial Biodiversity Far Eastern Branch of Russian Academy of Sciences, Vladivostok 690022, Russia*

*** Correspondence:**

Corresponding Author:

Xiaodan Yu

yuxd126@126.com

Lidiya Alekseevna Sibirina

sibirina@biosoil.ru

[#] **Co-authors**: Hongbo Guo and Weiye Liu are contributed equally to this work.

Keywords: shiro soil, ectomycorrhizal fungi, *Quercus mongolica*, rhizosphere microorganisms, symbiotic system, *Tricholoma bakamatsutake*

Abstract

Tricholoma bakamatsutake is a delicious and nutritious ectomycorrhizal fungus. However, its cultivation is hindered owing to limited studies on its symbiotic relationships. Hence, we aimed to investigate its symbiotic relationships with *Quercus mongolica*-*T. bakamatsutake*-associated bacteria and the physicochemical properties and microbiome of its rhizosphere. In this study, *T. bakamatsutake* shiro soil (Tb group) and corresponding *Q. mongolica* rhizosphere soil (CK group) samples were collected from different areas and analyzed for their physicochemical properties and microbiome structure. The Tb group samples had significantly higher sand content and lower levels of total and available phosphorus than those in the CK group soil samples. The microbiome analysis revealed that *T. bakamatsutake* within the symbiotic system had a significant dominant effect, altering its shiro microbiome structure by suppressing other microorganisms, such as *Russula*, another ectomycorrhizal fungus, and *Penicillum*, a phytopathogenic bacteria. The accompanying bacteria, including mycorrhizal-helper bacteria and plant growth-promoting bacteria, were

aggregated. Moreover, the microbiome in the symbiotic system was significantly involved in the catabolism of sugars and fats. Our findings elucidated the microbial community and relevant symbiotic environment to further understand the relationship between *T. bakamatsutake* and *Q. mongolica*.

1 Introduction

Tricholoma bakamatsutake, an edible mushroom, often forms ectomycorrhizae with the roots of Fagaceae trees, such as *Quercus mongolica* (Deng 2003; Ota et al. 2012). *T. bakamatsutake* has a similar appearance, smell, and nutritional value to that of *T. matsutake* (Quan et al. 2005, 2007); however, its commodity price is lower than that of *T. matsutake* (Kang et al. 2018). Market demand for *T. bakamatsutake* is increasing; however, yet its natural sources are limited. Therefore, cultivating *T. bakamatsutake* is necessary (Deng 2019; Hou 2020). Hence environmental conditions for the laboratory culture of *T. bakamatsutake* mycelia are being studied (Terashima 1994, 1999; Wu et al. 2009; Yamanaka et al. 2019), with researchers attempting to obtain fruiting bodies by transplanting the mycelia into natural environments (Hou 2020; Kawai et al. 2018). However, natural environments differ from laboratory environments and factors, such as soil physicochemical properties and the microbiome, may affect the yield of the fruiting bodies in the natural environment.

T. bakamatsutake has dense underground mycelia that form a white, sponge-like structure known as shiro (Ogawa 1977). In *T. matsutake,* the shiro plays an important role in the formation of fruiting bodies (Yun et al. 1997), which form at the core of the shiro. Metagenomic analysis using high-throughput sequencing has been frequently applied to study the microbiome in the shiro (Kim et al. 2014; *Oh* et al. 2016; Ye et al. 2018). The technique enables the discovery of unknown microbial diversity, including non-culturable microorganisms, by directly recovering genetic material from shiro samples for an intuitive analysis and comprehensive understanding of the microbiome structure (Kim et al. 2014; Shokralla et al. 2012). Kim et al. (2014) studied the bacterial community in *T. matsutake* shiro using pyrophosphate sequencing to show that environmental factors may influence the bacterial community more than the dominance of *T. matsutake* may influence the bacterial community. Oh et al. (2016) identified a number of *T. matsutake*-related microorganisms, such as *Bacillus* and *Umbelopsis,* which may exploit or aid *T. matsutake*. Vaario et al. (2011) reported that *T. matsutake* coexisted with diverse fungal and actinobacterial species and high enzyme activity is involved in the degradation of organic carbon in the shiro. Similarly, this approach is applicable to studying *T. bakamatsutake* shiro, which can provide insight into the growth patterns and communal relationships of *T. bakamatsutake* and lay a foundation for the future cultivation of *T. bakamatsutake* by inducing shiro degradation. Moreover, *T. bakamatsutake* adapts more easily to the environment than *T. matsutake* does and is therefore suitable for artificial cultivation (Deng 2019; Hou 2020). However, studies on *T. bakamatsutake* shiro are limited; thus, hindering its artificial cultivation and economic prospects.

T. bakamatsutake is an ectomycorrhizal (ECM) fungus. Therefore, its effects on other ECM fungi, host plants, and the environment require consideration. ECM fungi colonize plant roots and expand their shiro by altering the soil microbiome structure (Calvaruso et al. 2007; Li et al. 2019), thereby dominating their environment. The mechanisms underlying ECM fungi dominance include ecological niche competition, metabolite secretion, and mycorrhization helper bacteria (MHB) enrichment (Poole et al. 2001; Moeller and Peay 2016). The symbiotic relationship between ECM fungi and host plants is important; ECM fungi mycelia adhere closely to plant roots, effectively protecting woody plants from pathogens (Tedersoo et al. 2020). This symbiotic relationship improves nutrient exchange between ECM fungi and the plants. Plants transport photosynthates to the roots where ECM fungi are located, whereas ECM fungi transport minerals to the plant via mycorrhiza

(Nehls et al. 2010, 2018). Additionally, ECM fungi play important roles in increasing plant resilience and improving forest environments (Song et al. 2015; Bennett et al. 2017; Yu and Yuan 2023).

This study aimed to aid in the artificial cultivation of *T. bakamatsutak*e by examining the dominant effect of *T. bakamatsutak*e on the shiro and microorganisms associated with the growth and dispersal of its mycelia. Further, we evaluated the contribution of *T. bakamatsutak*e to the symbiotic system of the host and environment.

2 Materials and methods

2.1 Sample collection

In August 2022, 28 soil samples were collected from four cities in Liaoning Province, China. These 28 samples included 14 Tb and 14 corresponding CK samples, which were collected in a similar manner. The Tb samples were collected from the shiro soil under the fruiting body of *T. bakamatsutake*, and CK samples from the rhizosphere soil of *Q. mongolica* located 5 m outside the shiro. Their contents are presented in **Table 1**. Each sample was mixed and divided into three parts: the first was dried and passed through a 20-mesh sieve for determining chemical properties; the second was dried and passed through a 100-mesh sieve for determining mechanical composition; and the third was stored at –80 °C for DNA extraction.

2.2 Analysis of soil physicochemical properties

Soil physicochemical properties were analyzed at the Analytical and Testing Center of Shenyang Agricultural University. The standards for the physicochemical properties were: pH value: NY/T 1121.2-2006; total nitrogen (TN): NY/T 53-1987; total potassium (TK): NY/T 87-1988; total phosphorus (TP): NY/T 88-1988; available nitrogen (AN): DB13/T 843-2007; available potassium (AK): NY/T 889-2004; available phosphorus (AP): NY/T 1121.7-2014; organic matter (OM): NY/T 1121.6-2006; and soil machinery composition: NY/T 1121.3-2006.

2.3 DNA extraction, polymerase chain reaction (PCR) amplification, and Illumina MiSeq sequencing

Total genomic DNA of the microbiome was extracted using the E.Z.N.A.® soil DNA kit (Omega Bio-tek, Norcross, GA, USA) according to the manufacturer's instructions. The quality of the extracted genomic DNA was determined using 1% agarose gel electrophoresis, while its concentration and purity were determined using a NanoDrop 2000 (Thermo Fisher Scientific, Waltham, MA, USA).

For bacteria, 16S-specific primers 338F (5'-ACTCCTACGGGAGGCAGCAG-3') and 806R (5'-GGACTACHVGGGTWTCTAAT-3') were used to amplify different regions of the 16S ribosomal RNA (rRNA) gene. For fungi, specific primers, internal transcribed spacer ITS1F (5'-CTTGGTCATTTAGAGGAAGTAA-3') and ITS2R (5'-GCTGCGTTCTTCATCGATGC-3') were used to amplify different regions of the ITS gene. The PCR reactions were performed as previously described (Zhang Y. et al. 2020). The PCR products were extracted using 2% agarose gel and purified using the AxyPrep DNA Gel Extraction Kit (Axygen Biosciences, Union City, CA, USA) according to manufacturer's instructions and then quantified using a Quantus™ Fluorometer (Promega, Madison, WI, USA).

Purified PCR amplicons were pooled in equimolar amounts, paired-end, and sequenced on an Illumina MiSeq PE300 platform (Illumina, San Diego, CA, USA), according the Majorbio Bio-Pharm Technology Co. Ltd. (Shanghai, China) protocol. Raw sequencing reads were deposited in the database of the National Center for Biotechnology Information Sequence Read Archive (BioProject: PRJNA955660).

2.4 Data processing

Raw FASTQ files were de-multiplexed using an in-house perl script, quality-filtered using fastp version 0.19.6 (Chen et al. 2018), and merged using FLASH version 1.2.7 (Magoč and Salzberg 2011). The optimized sequences were clustered into OTUs using UPARSE 7.1 (Edgar 2013; Stackebrandt and Goebel 1994) with a 97% sequence similarity level. The most abundant sequence in each OTU was selected as the representative sequence. The taxonomy of each OTU representative sequence was analyzed using RDP Classifier version 2.2 (Wang et al. 2007) against the Silva 16S rRNA and Unite ITS gene databases with a confidence threshold of 0.7. Finally, metagenomic functions were predicted for bacterial and fungal communities. The functions of the bacterial community were predicted using PICRUSt2, FAPROTAX, and BugBase based on OTU representative sequences. Functions of the fungal communities were predicted using PICRUSt2 and FunGuid.

2.5 Statistical analysis

Data analysis was performed on the Majorbio Cloud platform (https://cloud.majorbio.com). Mothur (Schloss et al. 2009) software (http://www.mothur.org/.com/calculators) was used to calculate the alpha diversity indices, such as Chao and Shannon's indices. The Wilcoxon rank-sum test was used for inter-group variation analysis of the alpha diversity indices, and NMDS analysis based on the Bray-Curtis distance algorithm was used to test the similarity between the samples' microbial community structure. CCA and RDA were used to investigate the interactions between the soil physicochemical indicators and microbial community structure. To detect differences between the samples and overall differences and exclude chance data, the significant differences between the two groups were analyzed using a multiple-group sample analysis (eight groups) and two-group analysis of Tb and CK. The means of the differences in the physicochemical properties of the samples were determined using Duncan's multiple range test of variance and t-tests on SPSS Statistics software (version 17.0; IBM Inc., Armonk, NY, USA). The Kruskal-Wallis H test and Wilcoxon rank-sum test of variance were performed on the Majorbio Cloud platform.

3 Results

3.1 Physicochemical properties of the soil samples

The pH range of all the soil samples was 5.04–6.19. The results of the multigroup and two-group analyses showed that the two groups differed significantly based on physicochemical properties (**Table 2 and Supplemental Table 1**). The available phosphorus AP, TP, TN, and silt values for *T. bakamatsutake* shiro soil (Tb) group samples were lower than those of the *Q. mongolica* rhizosphere soil (CK) group. The TK and sand were higher in Tb than in those of CK samples.

3.2 Microbial genome annotation and alpha diversity indices of the microbiome

The raw data results from MiSeq for fungal community and bacterial community are presented in **Supplemental Tables 2 and 3**. Sample sequences were drawn flat according to the minimum

number of sample sequences before analysis. The fungal and bacterial coverage indices were 99.57–99.93% and 96.70–98.76%, respectively, after drawing flat. This indicated that most fungal and bacterial taxa were detected in the soil samples and the sequencing results depicted the microorganisms in the samples correctly.

Fungal alpha diversity indices were analyzed for significant differences (**Supplementary Figure 1**). For all regions, the Shannon index was significantly lower in the Tb group than in the CK group. Additionally, the Chao index was lower in the Tb group than in the CK group, indicating that the diversity of the fungal communities was significantly lower in the Tb group than in the CK group. In both groups, Xinbin (XB) Tb and XBCK had the lowest and highest Shannon and Chao indices, respectively. For bacteria, both the Shannon and Chao indices were higher in the Tb group than in the CK group, with significant differences in the Kuandian (KD) region. This indicates that bacterial community diversity increased in the Tb group.

3.3 Analysis of the microbiome structure

3.3.1 Fungal community

At the operational taxonomic unit (OTU) level (**Supplementary Figure 2a**), the Tb and CK groups shared 47 OTUs. These are common fungi found in the soil environment of oak forests. The number of unique OTUs was higher in the CK group than in the Tb group. The Tb group and the CK group (**Supplementary Figure 3**) were analyzed separately. The samples in the Tb group shared 63 OTUs, with XBTb and KDTb having the lowest (57) and highest (168) number of unique OTUs, respectively. All samples in the CK group shared 136 OTUs, with Anshan (AS)CK and Xiuyan (XY)CK having the highest (567) and lowest (92) number of unique OTUs, respectively. At the phylum level, Basidiomycota, Ascomycota, and Mortierellomycota were dominant in all soil groups. Basidiomycota (96.21–99.77%) and Ascomycota (56.02–83.65%) were the dominant phyla in the Tb and CK groups, respectively. At the genus level, the heatmap and abundance bubble map (**Figure 1**) indicated that *Tricholoma*, *Russula*, and *Mortierella* were the dominant fungal genera in the different regions. Except for *Tricholoma*, most genera in the Tb group were less abundant than those in the CK group. At the species level, *T. bakamatsutake* was the dominant species in the Tb group having 87.7, 88.0, 99.1, and 89.1% abundance in the AS, KD, XB, and XY regions, respectively.

3.3.2 Bacterial community

At the OTU level (**Supplementary Figure 2b**), 663 OTUs were shared between the Tb and CK groups. The Tb group had more unique OTUs than those in the CK group. A total of 1,674 OTUs were observed in the Tb group (**Supplementary Figure 4**). The most (536) and fewest (157) unique OTUs were observed in the XBTb and KDTb regions, respectively. A total of 1,039 OTUs were observed in the CK group (**Supplementary Figure 4**). The most (816) and fewest (163) unique OTUs were observed in the ASCK and XYCK regions, respectively. At the phylum level, Actinobacteria, Proteobacteria, and Acidobacteria were dominant in all soil groups. Proteobacteria and Actinobacteria were the most abundant phyla in the CK and Tb groups, respectively. The genus-level heatmap (**Figure 2a**) and abundance bubble map (**Figure 2b**) indicated that the genera *Bradyrhizobium*, *Acidothermus*, *Mycobacterium*, *norank_f__Xanthobacteraceae*, *Burkholderia-Caballeronia-Paraburkholderia* (BCP) were the dominant genera in both groups.

3.4 Analysis and comparison of the microbiome structure and significant differences in both groups

The non-metric multidimensional scaling (NMDS) analysis results showed differences in the microbiome structures in the CK and Tb groups. The fungal communities (**Supplementary Figure 5a**) in the CK and Tb groups differed. In the CK group, the KDCK region was far from the other CK regions, indicating that the structure of the fungal community of the oak forests in the KD region differed from those of other areas. The bacterial communities (**Supplementary Figure 5b**) in both groups were generally similarly distant, but different from each other.

The Kruskal-Wallis H test (eight groups) and Wilcoxon rank-sum test (CK and Tb) were used to analyze the differences in the abundance of microorganisms between the groups. In the fungal community (**Supplementary Figure 6**), *T. bakamatsutake* was significantly more abundant in the Tb group than in the CK group, whereas almost all other fungi, such as *Russula* and *Penicillium*, were significantly lower in abundance in the Tb group than in the CK group. This suggests that the dominance of Tb has a broad and significant effect on other fungi. The dominance of one species did not result in an overwhelming change in the bacterial community. In the Tb group (**Supplementary Figure 7**), a significant increase in the Actinobacteria, such as *norank_f__67-14*, *Streptomyces*, *Pseudonocardia, Bradyrhizobium, norank_f__Xanthobacteraceae*, *norank_f__norank_o__Elsterales*, *Bryobacter*, and other genera were significantly lower in the Tb group than in the CK group. The multi-group analysis results showed that BCP was significantly more abundant in the ASTb and XYTb regions than in the corresponding CK group regions, and less abundant in the KDTb and XBTb regions than in the corresponding CK group region, a phenomenon that may not be by chance. We further focused on the abundance of common MHB (Frey-Klett et al. 2007) for the analysis (**Supplementary Figure 8**). The MHB identified, which were significantly more abundant in the Tb group than in the CK group, were *Sphingomonas*, *Paenibacillus,* and *Bacillus*.

3.5 Correlation between environmental factors and microorganism levels

Based on the canonical correspondence analysis (CCA)/ redundancy analysis (RDA) correlation between environmental factors and the fungal and bacterial communities (**Figure 3**), environmental factors that had significant effects on the fungal community, including AP, TP, TN, sand, silt, and silt with sand, were positively correlated with Tb samples. Environmental factors that had a significant effect on bacterial communities, including AK, AP, TK, TP, TN, sand, silt, and silt with sand and TK, were significantly positively correlated with most Tb samples.

According to the Spearman analysis results(**Figure 4**) , fungal and bacterial communities had almost identical correlation trends between *T. bakamatsutake* soil physicochemical properties and a few Actinobacteria genera, which were almost all positively correlated with clay, TK, and sand, and negatively correlated with other physicochemical factors.

3.6 Functional prediction of microorganisms

Functional predictions were made for the bacterial and fungal communities, and the number of enzymes and pathways is explained in **Supplemental Table 4**. The fungal community function was predicted using Phylogenetic Investigation of Communities by Reconstruction of Unobserved States (PICRUSt2) and FunGuid. The results of the enzyme-level analysis of Kyoto Encyclopedia of Genes and Genomes (KEGG) function indicated that adenosine triphosphatase, glucan 1,4-alpha-glucosidase, and unspecific monooxygenase were the most abundant across the samples. MetaCyc pathway abundance statistics showed that aerobic respiration I, aerobic respiration II, fatty acid, and beta oxidation were the most abundant metabolic pathways in each sample. To analyze the significant differences, we focused on the top 50 data points on abundance. The results showed that the abundance of enzymes (**Supplementary Figure 9a and c**), such as glucan 1,4-α-glucosidase and

carboxylesterase, and metabolic pathways (**Supplementary Figure 9b and d**), such as aerobic oxidation and fatty acid degradation, were significantly more in the Tb group than in the CK group. Fungal communities were classified using the fungal FunGuid function and its results showed that ectomycorrhizal fungi (including ectomycorrhizal and ectomycorrhizal-fungal parasites) were the most abundant fungi in all groups. Analysis of the significance of these differences (**Supplementary Figure 10a and b**) showed that ectomycorrhizal-fungal parasites were significantly higher in the Tb than in the CK group, whereas ectomycorrhizal and saprotrophic parasites were significantly lower in the Tb than in each of the CK groups.

Functional prediction of bacterial communities was performed using PICRUSt2, BugBase, and FAPROTAX. Enzyme-level analysis of KEGG function showed that NADH: ubiquinone reductase, DNA-directed DNA polymerase, and DNA helicase were the most abundant across the samples. MetaCyc pathway abundance statistics showed that aerobic respiration I and pyruvate fermentation of isobutanol were the most abundant pathways in each sample. Analysis of significant differences showed that these enzymes (**Supplementary Figure 11a and c**), such as enoyl-CoA hydratase and long-chain-fatty-acid-CoA ligase, and metabolic pathways (**Supplementary Figure 11b and d**), such as fatty acids, beta, and-oxidation I, were significantly more abundant in the Tb group than in the CK group. The bacteria were phenotypically predicted using BugBase and analyzed for significant differences (**Supplementary Figure 12**). The results showed that seven of the nine phenotypes differed significantly. The phenotypes that were most frequent in the Tb group were gram-positive, contained mobile elements, and stress-tolerance, whereas the phenotypes that were more frequent in the CK group were facultative, anaerobic, potentially pathogenic, gram-negative, and aerobic. The metabolic and ecological functions of the bacteria were predicted using FAPROTAX software. The results (**Supplementary Figure 13**) showed that chemoheterotrophy and aerobic chemoheterotrophs were the most abundant in each sample. The abundance of chemoheterotrophy, aerobic chemoheterotrophs, and aromatic compound degradation was higher in the Tb group than in the CK group, whereas nitrogen fixation was lower in the Tb group than in the CK group.

4 Discussion

4.1 Physicochemical properties of *T. bakamatsutake* shiro

The pH value range for all samples was between 5.04 and 6.19, which is optimal for the growth of most ECM fungi (Yamanaka 2003); therefore, ECM was most abundant in both the Tb and CK groups. The TP and AP levels were significantly lower in the Tb group than in the CK group. TP most likely forms AP through phosphorus solubilization in *T. bakamatsutake* soil, whereas AP is passed on to oak through symbiotic nutritional relationships.

Sand content was significantly higher in the Tb group than in the CK group, whereas silt content was significantly lower in the Tb group than in the CK group. This result is similar to that of the soil structure of the *T. matsutake* habitat (Ji et al. 2022). Improved air and water permeability in the soil may be necessary for the survival of *T. bakamatsutake*. The relationship between the physicochemical properties and microorganisms was determined using subsequent correlation analysis.

4.2 *T. bakamatsutake* alters microbiome diversity

The fungal diversity in the *T. bakamatsutake* shiro was significantly lower than that in the ambient soil in almost every region. This indicates that *T. bakamatsutake* has an absolute dominant

effect on its shiro, which reduces or eliminates other fungi, thereby reducing the diversity of the fungal community. The fungal diversity in the XBTb region is lower than that of the other areas in the Tb group because the XB sampling site is abundant in *T. bakamatsutake* and its dominance produces a significant impact. Fungal diversity was highest in XBCK among all the samples, suggesting that the soil environment in XB is suitable for a wide range of fungi. Thus, the XB environment is favorable for the growth of *T. bakamatsutake*.

For the bacterial community, all Tb groups had higher bacterial diversity than that of the corresponding CK groups. ECM fungi roots can support different types of bacteria (Liu et al. 2018), as the expanded mycelial network of the ECM fungi provides a habitat for bacterial communities (Miquel et al. 2018), and the photosynthetic products obtained from the ECM fungi provide nutrition for many bacteria (*Colin* et al. 2017; *Read and Perez-Moreno 2003; Van Schöll et al. 2006*). In our study, *T. bakamatsutake* received most carbohydrates from the plants and its mycelia expanded in a denser network, attracting various types of bacteria.OM degraded or secreted by *T. bakamatsutake* may cause bacterial aggregation; however, the exact substances need to be confirmed.

4.3 Bacterial community analysis

4.3.1 MHB and endophytic bacteria associated with *T. bakamatsutake*

MHB can increase mycorrhization by inducing the rapid expansion of fungal mycelia and stimulating the formation of plant lateral roots to increase contact opportunities (*Riedlinger et al. 2006;* Rigamonte et al. 2010). Mycorrhizal fungi are selective regarding the type of bacteria in their rhizosphere (Izumi and Finlay 2011), with different mycorrhizal fungi selecting different bacteria based on their requirements. In our study, *Sphingomonas*, *Paenibacillus,* and *Bacillus* had high abundance and were significantly different between the Tb group and CK group. These bacteria, often found in mycorrhizal environments (*Bending* et al. 2002; *Timonen and Hurek 2006; Nguyen and Bruns 2015*), promote the growth and colonization of ectomycorrhizal mycorrhizae (Ji et al. 2022; *Requena* et al. 1997; *Hrynkiewicz* et al. 2009). Species of the genera *Bacillus* and *Paenibacillus* were significantly high in abundance in the *T. matsutake* shiro (*Oh et al. 2016*). *Sphingomonas* are endophytic bacteria in the ECM, such as *T. matsutake* cotyledons (Liu et al. 2021), which possess the ability to degrade aromatic compounds and exhibit metabolic activity against toxic pollutants (Yang et al. 2022). Thus, several of the above-mentioned bacteria may contribute to the growth and development of *T. bakamatsutake* and its root-colonizing mycelia.

4.3.2 *T. bakamatsutake* aggregated plant growth-promoting bacterium (PGPB)

In our study, bacterial genera that have been confirmed as PGPB, such as BCP, *Solirubrobacter*, and *Bacillus*, were significantly more abundant in the Tb group than in the CK group. In future studies, several genera with high abundances will be explored. BCP are widely distributed in the soil and plant roots and promote plant growth, improve plant resistance, and reduce self-toxicity (Luo et al. 2021; Beukes et al. 2017). In our study, BCP abundance was higher in both the ASTb and XYTb samples than in the corresponding CK samples. Inter-root secretions are enriched with and degraded by BCP to reduce plant auto-toxicity (Luo et al. 2021). Therefore, the possibility of Tb inter-root secretions, whether enriched with BCP or not, requires further study.

In addition to being beneficial to plants, BCP aid the development of *T. matsutake* (Xu 2021). Actinobacteria are considered special PGPB that promote plant growth and help plants resist pathogenic bacteria in several ways, including the decomposition of OM, secretion of antibiotics, degradation of pollutants, and secretion of phytohormones (Bhatti et al. 2017; Olanrewaju and

Babalola 2019; Hayat et al. 2021). In our study, the relative abundance of Actinobacteria was significantly higher in Tb samples than in CK samples. The significant increase in Actinobacteria was mainly concentrated in the genera *Streptomyces*, *Pseudonocardia*, *norank_f__67-14*, *Nocardioides*, and *Solirubrobacter*. *Streptomyces,* the most highly anticipated PGPB among actinomycetes*,* can efficiently colonize the inter-root surfaces and promote plant growth through the direct production of phytohormones and the decomposition of OM (Olanrewaju and Babalola 2019; Verma et al. 2011). *Norank_f__67-14* and *Solirubrobacter* species belong to the order Solirubrobacterales, which increase phosphorus flow and inhibit the flow of toxic aluminum and manganese from the soil to the plant, thereby promoting high crop yields (Wang et al. 2022). *Nocardioides* and *Pseudonocardia* are highly metabolically active against toxic pollutants and their secretions have antimicrobial activity (Yang et al. 2022; Carr et al. 2012; Singha and Pandey 2021). Therefore, *T. bakamatsutake* aggregates Actinobacteria to degrade soil contaminants, secrete antibiotics to suppress pathogenic bacteria, and provide nutrients for itself, thereby aiding in growth and development of itself and that of the oak environment.

4.3.3 Interactions among the bacteria in *T. bakamatsutake* shiro

Microorganisms interact via metabolites. In our study, actinomycetes had the most significant effect on other bacteria, especially gram-negative bacteria. The abundance of *norank_f__norank_o__Elsterales* was lower in the Tb group than in the CK group. Elsterales may be associated with plant pathogenicity, soil carbon metabolism, aluminum accumulation, and soil impoverishment (Xu 2021). This suggests that actinomycetes can suppress microorganisms that are detrimental to *T. bakamatsutake* and oak forests.

However, actinomycetes can inhibit beneficial microorganisms, such as the BCP. The analysis of the significant differences in the bacterial communities and Spearman's analysis (**Supplementary Figure 14**) showed that Actinobacteria, *Pseudonocardia*, *Solirubrobacter*, and *Nocardioides,* were significantly and negatively correlated with BCP, with significant differences in the abundance of the three genera in XB and KD. Nocardicin A, a metabolite of *Nocardioides*, has a broad-spectrum gram-negative inhibitory effect (Aoki et al. 1976; Nishida et al. 1977; Luo et al. 2014) and is a natural product of *Pseudonocardia* (Carr et al. 2012). Therefore, bacteria that belong to BCP genera may be more sensitive than other bacteria are to the inhibitory effects of these three genera. This explains the low abundance of the BCP in XBTb and KDTb. Other beneficial bacteria, such as *Bryobacter* (Wang et al. 2022) and *Roseiarcus* (Yu et al. 2020) were similarly significantly affected. Despite the inhibitory effects of actinomycetes, beneficial bacteria still prevailed, and some of which, such as *Bacillus* were not as negatively affected; therefore, this did not affect the growth and development of *T. bakamatsutake*.

Bacterial competition for ecological niches was considered in our study. *Bradyrhizobium* and *norank_f__Xanthobacteraceae*, which are nitrogen-fixing rhizobia (Rhizobiales) that promote the growth and root development of some plants (Yang et al. 2022), were highly abundant in all samples. Therefore, Rhizobiales are *T. bakamatsutake* symbionts; however, they were lower in the Tb samples than in the corresponding CK samples, which is very significant. In addition to antibiotic antagonism, Rhizobiales compete with other bacteria, such as *Frankia* (Wall 2000) for nitrogen fixation, ecological niches, and other aspects.

The interactions between bacterial communities are not limited to antagonistic and competitive interactions, and symbiotic interactions were observed in our study. A prime example is the manner in which actinomycetes suppress some bacteria and degrade many toxic pollutants to provide nutrients and a good habitat for other bacteria and plants. These effects are not as widespread as the antagonistic effects of actinomycetes; however, they were apparent.

4.4 Fungal community analysis

4.4.1 Effect of *T. bakamatsutake* on other fungi

T. bakamatsutake dominated its shiro, with the highest relative abundance of 99.1% in XBTb. Most fungi in the Tb group were affected by the dominant effect of *T. bakamatsutake*; therefore, we divided the fungi affected by *T. bakamatsutake* into two main groups. The first group comprised other ECM fungi that mainly included *Russula*, *Piloderma*, *Laccaria*, and *Sebacina*. The dominant effect of *T. bakamatsutake* on other ECM fungi is reflected in the competition for ecological niches, such as plant root symbiosis sites and soil nutrients, whereas *T. bakamatsutake* metabolites may have a suppressive effect on other ECM fungi. The second group included reported plant pathogenic fungi such as *Penicillium* (Li et al. 2010) and *Trichoderma* (Gajera et al. 2015). The dominant effect of *T. bakamatsutake* on pathogenic fungi is reflected in the competition for nutrients and survival space, while actinomycetes enriched by *T. bakamatsutake* inhibit some pathogenic fungi. In addition to these two groups of fungi, other common fungi in oak forests were affected by the dominance of *T. bakamatsutake*.

4.4.2 Characteristics of the *T. bakamatsutake* habitat

The fungal communities in the CK group from the four areas were analyzed jointly (**Figure 5**). We found that ECM fungi, such as *Russula*, *Piloderm,* and *Lactifluus* shared a similar habitat with *T. bakamatsutake*—the oak forest. However, these ECM fungi are the main competitors of *T. bakamatsutake*, the most competitive being *Russula*, which is the most abundant among the ECM fungi (Ji et al. 2019). In addition to mycorrhizal fungi, genera, such as *Mortierella* are common fungi present under oak trees, which may contribute to the growth of oak forests (Guo et al. 2022) and indirectly help the formation of symbiotic relationships between oak forests and mycorrhizal fungi.

4.5 The potential function of *T. bakamatsutake* in relation to *Q. mongolica*

We made preliminary predictions about the function of *T. bakamatsutake* by comparing the function of the fungi in the Tb group with that in the CK group. In the predicted results for MetaCyc pathways, we found a significantly high abundance of pathways related to sugar and lipid catabolism in the Tb group. For example, aerobic respiration I, tricarboxylic acid cycle II, glycolysis III, pentose phosphate pathway, and fatty acid beta-oxidation were significantly higher in the Tb group than in the CK group. As a member of ECM fungi, *T. bakamatsutake* derives nutrients mainly from the host plant sugars and fats for its own nutritional development (Nehls et al. 2010). Therefore, *T. bakamatsutake*'s function is related to the catabolism of sugars and fats. Notably, the glyoxylate cycle was significantly more abundant in the Tb group than in the CK group. This may indicate that the source of sugars in *T. bakamatsutake* is not only supplied directly by the host plant, but some may be derived from sugars formed by acetyl CoA through the glyoxylate cycle and other pathways. Additionally, octane oxidation was significantly higher in the Tb group than in the CK group. The application of microbial degradation of aromatic hydrocarbons is of great value; however, studies on the degradation of aromatic compounds by mycorrhizal fungi are limited. Our results indicate that *T. bakamatsutake* may be a new direction.

To predict enzyme levels for KEGG functional abundance based on the PICRUSt2 function, we focused on the abundance of a number of enzymes with high and variable abundance. Glucan 1,4-alpha-glucosidase was the most abundant in the Tb group, and the 1,4-alpha glycosidic bond was mostly present in starch, which is related to the function of *T. bakamatsutake* in the breakdown of sugars, such as starch. Carboxylesterase was significantly more abundant in the Tb group than in the CK group, and this enzyme hydrolyzed tannins and corneum from the cell wall. The corneum is a

hydroxy fatty acid mixed with wax on the outside of the cell wall to form the cuticle (Samuels et al. 2008; Arya et al. 2021). The ECM fungi adheres closely to the host roots and secretes cell wall-degrading enzymes to remodel the cell wall, forming a Hartig net that expands the interface for nutrient exchange with the plant (Yu and Yuan 2023). The plant cuticle is a barrier against microbial infestation (Yeats and Rose 2013; Ziv et al. 2018); hence, the role of carboxylesterases from *T. bakamatsutake* may be reflected in their association with host plant root cells. Chitinase abundance was significantly high in the Tb group. Chitinase degrades the fungal cell wall and releases spores, a phenomenon that is often observed in ECM fungi. The abundance of gibberellin 2-beta-dioxygenase, an enzyme involved in gibberellin anabolism, was also increased in the Tb group. This may have a facilitative and regulatory role for plant hosts in the habitat and for the growth of *T. bakamatsutake*. Choline dehydrogenase can oxidize choline, which is subsequently oxidized by the enzyme betaine-aldehyde dehydrogenase to form betaine (Zhang Y.J. et al. 2020); however, the latter was in low abundance in the Tb group. Additionally, enzymes such as tripeptidyl-peptidase I and non-specific monooxygenase were also significantly high in abundance in the Tb group, which may provide us with interesting findings in the future.

4.6 Changes in the function of mycorrhizal bacterial communities

4.6.1 Prediction of bacterial function using PICRUSt2

At the enzyme level, the abundance of enzymes involved in fatty acid and sugar catabolism, such as enoyl-CoA hydratase, long-chain-fatty-acid-CoA ligase, pyruvate dehydrogenase, and dihydrolipoyl dehydrogenase, was significantly higher in the Tb group than in the CK group. The abundance of metabolic pathways, such as fatty acid beta-oxidation I, was also significantly high in the Tb group. Hence, Tb group soils may be enriched with bacteria related to fatty acid and sugar catabolism. Additionally, the abundance of betaine-aldehyde dehydrogenase at the enzyme level was significantly higher in the Tb group than in the CK group, suggesting that in the Tb group, the bacterial community may fill the gap in the fungal community with less abundance of this enzyme, and perhaps a collaborative effect between the fungus and bacteria exists for improved betaine formation.

4.6.2 Prediction of bacterial phenotypes using BugBase

The main factor contributing to the significantly different BugBase phenotypes of the bacterial communities was the aggregation of actinomycetes in Tb. The inhibitory effect of the actinomycetes on gram-negative bacteria may be more pronounced such that more gram-positive and fewer gram-negative bacteria than those in the CK group were observed in the Tb group. The significantly high stress-tolerance phenotype in the Tb group may be related to antibiotic stress resistance, as fewer non-resistant bacteria were inhibited in Tb. The possibility that the bacterial community in the Tb group had high stress tolerance cannot be ruled out. Further, the relative abundance of potentially pathogenic bacteria was lower in the Tb group than in the CK group, and some plant pathogenic bacteria were included; therefore, the probability of pathogenic bacteria being attacked in Tb soils was low for both the plants and *T. bakamatsutake* itself.

4.6.3 Prediction of bacterial function using FAPROTAX

Both chemoheterotrophy and aerobic chemoheterotrophs were more abundant in Tb than in the CK group. The carbon and energy sources of chemoheterotrophic microorganisms originate from the oxidative decomposition of OM. Saprophytic bacteria were the most abundant among chemoheterotrophic bacteria. In the Tb group, *T. bakamatsutake* dominated and significantly reduced the abundance of saprophytic fungi. However, *T. bakamatsutake* had limited scope and efficiency in

decomposing OM; therefore, an increase in saprophytic bacteria is needed to compensate for the scope and efficiency of saprophytic functions in the Tb group. Nitrogen fixation was significantly reduced in Tb, possibly because of the antagonistic effects mentioned in the bacterial community and competition for ecological niches, resulting in a reduction in nitrogen-fixing bacteria such as *Bradyrhizobium*. Degradation of aromatic compounds was higher in the Tb group than in the CK group. Aromatic compounds can cause serious environmental pollution, and the significantly high abundance of aromatic compound-degrading bacteria in the Tb group were mainly from the several aforementioned actinomycetes. Plant pathogens were significantly less abundant in the Tb group than in the CK group, suggesting that some plant pathogenic bacteria were inhibited by Tb.

5 Conclusion

In this study, the diversity and population structure of microbiology in the soils of the Tb group and the CK group were compared using a microbiome approach. In the Tb group samples, *T. bakamatsutake* was the absolute dominant species, and the species diversity and other fungal species richness decreased significantly. On the contrary, bacterial diversity increased and bacterial community structure was changed in the Tb group compared with that of the CK group. There were more abundant PGPB and MHB in the Tb group than in the CK group. Abundant MHB (*Sphingomonas*, *Paenibacillus*, and *Bacillus*) promotes fungal hyphal growth and mycorrhizal formation. PGPB is capable of producing plant growth regulators, promoting plant growth, and improving resistance to drought and salt tolerance. The results showed that *T. bakamatsutake* not only directly provided water and minerals to *Q. mongolica*, but also promoted the growth of the host by regulating the soil microbial community structure (**Figure 6**). This study is important for constructing a healthy soil microbial community structure and cultivating *T. bakamatsutake-Q. mongolica* mycorrhizal seedlings.

TABLE 1. | Collection and grouping of the 28 soils samples.

Cities	*T. bakamatsutake* shiro soils	*Q. mongolica* rhizosphere soils
AnShan (AS)	ASTb1, ASTb2, ASTb3	ASCK1, ASCK2, ASCK3
KuanDian (KD)	KDTb1, KDTb2, KDTb3	KDCK1, KDCK2, KDCK3
XinBin (XB)	XBTb1, XBTb2, XBTb3, XBTb4, XBTb5	XBCK1, XBCK2, XBCK3, XBCK4, XBCK5
XiuYan(XY)	XYTb1, XYTb2, XYTb3	XYCK1, XYCK2, XYCK3

Tb: *T. bakamatsutake* shiro soil, CK: *Q. mongolica* rhizosphere soil. AS: Anshan (123°9'26"E, 41°0'13"N, 267 m), KD: Kuandian (124°53'0"E, 41°30'15"N, 323 m); XB: Xinbin (125°24'5"E, 41°36'54"N, 662.94 m); XY: Xiuyan (123°41′35″E, 40°19'13"N, 254.53 m).

TABLE 2. | Physicochemical properties of *Tricholoma bakamatsutake* shiro soils.

Sample	AK (mg/kg)	AP (mg/kg)	AN (mg/kg)	TK (%)	TP (%)	TN (%)	OM (g/kg)	pH	Sand (%)	Silt (%)	Clay (%)
ASTb	142.6e	1.133f	252.10f	2.41a	0.069e	0.402e	108d	5.41d	57.333a	28.00e	14.667d
ASCK	161.8c	2.60e	215.80g	2.13b	0.087a	0.489a	116c	5.66c	48.00b	37.00c	15.00c,d
KDTb	127.6f	3.40d	322.10c	1.63d	0.059g	0.412d	122b	5.31e	49.333b	33.333d	17.333b,c,d
KDCK	157.8d	5.50b	302.20d	1.33f	0.072d	0.452c	116c	5.81b	34.00c	47.00a	19.00a,b,c
XBTb	36.4h	2.70e	283.10e	1.39e	0.065f	0.348f	106d	5.24e	36.00c	42.00b	22.00a
XBCK	124.6g	6.50a	327.70b	1.21g	0.079b	0.461b	117c	6.19a	35.00c	50.00a	15.00c,d
XYTb	252.6a	3.30d	348.20a	1.78c	0.054h	0.398e	136a	6.17a	60.00a	30.00e	10.00e
XYCK	176.8b	4.80c	283.10e	1.23g	0.075c	0.413d	121b	5.04f	30.00d	50.00a	20.00a,b

Values are presented as the means of three replicates. Means in a column followed by different letters are significantly different at $P \leq 0.05$ according to the Ducan's multiple range test.

6 Conflict of Interest

The authors declare that the research was conducted in the absence of any commercial or financial relationships that could be construed as a potential conflict of interest.

7 Funding

This study was supported by Science and Technology Plan Project of Liaoning Province (2022-MS-418) and the National Natural Science Foundation of China (32370008).

8 References

Aoki, H., Sakai, H., Kohsaka, M., Konomi, T., Hosoda, J. (1976). Nocardicin A, a new monocyclic beta-lactam antibiotic. I. Discovery, isolation and characterization. *The Journal of Antibiotics*, 29, 492–500. doi: 10.7164/antibiotics.29.492

Arya, G.C., Sarkar, S., Manasherova, E., Aharoni, A., Cohen, H. (2021). The Plant Cuticle: An Ancient Guardian Barrier Set Against Long-Standing Rivals. *Frontiers in Plant Science*, 12, 663165. doi: 10.3389/fpls.2021.663165

Bending, G.D., Poole, E.J., Whipps, J.M., Read, D.J. (2002). Characterisation of bacteria from *Pinus sylvestrisa-Suillus luteus* mycorrhizas and their effects on root-fungus interactions and plant

growth. *FEMS Microbiology Ecology*, 39, 219–227. doi: 10.1111/j.1574-6941.2002.tb00924.x

Bennett, J.A., Maherali, H., Reinhart, K.O., Lekberg, Y., Hart, M.M., Klironomos, J. (2017). Plant-soil feedbacks and mycorrhizal type influence temperate forest population dynamics. *Science*, 355, 181–184. doi: 10.1126/science.aai8212

Beukes, C. W., Palmer, M., Manyaka, P., Chan, W. Y., Avontuur, J. R., van Zyl, E., Huntemann, et al. (2017). Genome Data Provides High Support for Generic Boundaries in *Burkholderia* Sensu Lato. *Frontiers in microbiology*, 8, 1154. doi: 10.3389/fmicb.2017.01154

Bhatti, A.A., Haq, S., Bhat, R.A. (2017). Actinomycetes benefaction role in soil and plant health. *Microbial Pathogenesis*, 111, 458–467. doi: 10.1016/j.micpath.2017.09.036

Calvaruso, C., Turpault, M.P., Leclerc, E., Frey-Klett, P. (2007). Impact of ectomycorrhizosphere on the functional diversity of soil bacterial and fungal communities from a forest stand in relation to nutrient mobilization processes. *Microbial Ecology*, 54, 567–577. doi: 10.1007/s00248-007-9260-z

Carr, G., Derbyshire, E.R., Caldera, E., Currie, C.R., Clardy, J. (2012). Antibiotic and antimalarial quinones from fungus-growing ant-associated *Pseudonocardia sp*. *Journal of Natural Products*, 75, 1806–1809. doi: 10.1021/np300380t

Chen, S., Zhou, Y., Chen, Y., Gu, J. (2018). fastp: an ultra-fast all-in-one FASTQ preprocessor. *Bioinformatics*, 34, i884–i890. doi: 10.1093/bioinformatics/bty560

Colin, Y., Nicolitch, O., Turpault, M. P., Uroz, S. (2017). Mineral Types and Tree Species Determine the Functional and Taxonomic Structures of Forest Soil Bacterial Communities. *Applied and environmental microbiology*, 83(5), e02684-16. doi: 10.1128/AEM.02684-16

Deng, H. (2003). Overview of research on *Tricholoma bakamatsutake* in China. Proceedings of the Third Congress of the Chinese Society of Mycology and the Sixth National Symposium on Mycology, 138–142.

Deng, Z.Z. (2019). Advances in the study of *Tricholoma bakamatsutake*. *Agricultural Science & Technology and Equipment*, 2, 19–20+24. doi: 10.16313/j.cnki.nykjyzb.2019.02.009

Edgar, R.C. (2013). UPARSE: highly accurate OTU sequences from microbial amplicon reads. *Nature Methods*, 10, 996–998. doi: 10.1038/nmeth.2604

Frey-Klett, P., Garbaye, J., Tarkka, M. (2007). The mycorrhiza helper bacteria revisited. *New Phytologist*, 176, 22–36. doi: 10.1111/j.1469-8137.2007.02191.x

Gajera, H.P., Savaliya, D.D., Patel, S.V., Golakiya, B.A. (2015). *Trichoderma viride* induces pathogenesis related defense response against rot pathogen infection in groundnut (*Arachis hypogaea* L.). *Infection, Genetics and Evolution*, 34, 314–325. doi: 10.1016/j.meegid.2015.07.003

Guo, P., Xing, P.J., Song, J., Wu, L.L., Li, B.Q., Si, Y.J., et al. (2022). Fungal community in roots and the root zone of *Quercus mongolica* and the correlations with the environmental factors. *Journal of Fungal Research*, 20, 173-182. doi: 10.13341/j.jfr.2022.1489

Hayat, S., Ashraf, A., Aslam, B., Asif, R., Muzammil, S., Asif Zahoor, M., et al. (2021). Actinobacteria: Potential Candidate as Plant Growth Promoters. IntechOpen. doi: 10.5772/intechopen.93272

Hou, J.W. (2020). Annotation of the Mitochondrial Genome of *Tricholoma bakamatsutake* and Comparison with Related Species. [Dissertation], [Shanxi]: Shanxi University

Hrynkiewicz, K., Christel, B., Niedojadło, J., Hanna, D. (2009). Promotion of mycorrhiza formation and growth of willows by the bacterial strain *Sphingomonas sp*. 23L on fly ash. *Biology and Fertility of Soils*, 45, 385–394. doi: 10.1007/s00374-008-0346-7

Izumi, H., Finlay, R.D. (2011). Ectomycorrhizal roots select distinctive bacterial and ascomycete communities in Swedish subarctic forests. *Environmental Microbiology*, 13, 819–830. doi: 10.1111/j.1462-2920.2010.02393.x

Ji, R.Q., Xing, P.J., Xu, Y., Li, G.L., Gao, T.T., Zhou, J.J., et al. (2019). Analysis of the composition of symbiotic fungal and bacterial in the roots and rhizosphere soil of *Quercus mongolica*. *Mycosystema*, 38, 1894-1906. doi: 10.13346/j.mycosystema.190181

Ji, R.Q., Xu, Y., Si, Y.J., Phukhamsakda, C., Li, Y., Meng, L.P., et al. (2022). Fungal-Bacterial Networks in the Habitat of SongRong (*Tricholoma matsutake*) and Driving Factors of Their Distribution Rules. *Journal of Fungi*, 8, 575. doi: 10.3390/jof8060575

Kang, J.A., Ka, K.H., Kim, J.Y., Kim, S.H. (2018). Mycelial Growth Properties of Domestically Collected Ectomycorrhizal *Tricholoma* Mushrooms in Various Culture Conditions. *The Korean Journal of Mycology*, 46, 271–280. doi: 10.4489/kjm.20180037

Kawai, M., Imaji, A., Yamada, A., Kinoshita, A. (2018). Shiro formation and fruitbody flflashing of *T. bakamatsutake* mycelia in the forest. In Abstracts of papers presented at the 62th annual meeting of the mycological society of Japan (Vol. 40) (in Japanese).

Kim, M., Yoon, H., Kim, Y.E., Kim, Y.J., Kong, W.S., Kim, J.G. (2014). Comparative analysis of bacterial diversity and communities inhabiting the fairy ring of *Tricholoma matsutake*

by barcoded pyrosequencing. *Journal of Applied Microbiology*, 117, 699–710. doi: 10.1111/jam.12572

Li, Q., Ning, P., Zheng, L., Huang, J., Li, G., Hsiang, T. (2010). Fumigant activity of volatiles of *Streptomyces globisporus* JK-1 against *Penicillium italicum* on Citrus microcarpa. *Postharvest Biology and Technology*, 58, 157–165. doi: 10.1016/j.postharvbio.2010.06.003

Li, X., Zhang, X., Yang, M., Yan, L., Kang, Z., Xiao, Y. (2019). *Tuber borchii* Shapes the Ectomycorrhizosphere Microbial Communities of *Corylus avellana*. *Mycobiology*, 47, 180–190. doi: 10.1080/12298093.2019.1615297

586 Liu, D., Pérez-Moreno, J., Zhang, P., Wang, R., Chater, C., Yu, F. (2021). Distinct
587 Compartmentalization of Microbial Community and Potential Metabolic Function in the
588 Fruiting Body of *Tricholoma matsutake*. *Journal of Fungi*, 7, 586–586. doi:
589 10.3390/jof7080586

590 Liu, Y., Sun, Q., Li, J., Lian, B. (2018). Bacterial diversity among the fruit bodies of ectomycorrhizal
591 and saprophytic fungi and their corresponding hyphosphere soils. *Scientific Reports*, 8, 11672.
592 doi: 10.1038/s41598-018-30120-6

593 Luo, L., Wang, L., Deng, L., Mei, X., Liu, Y., Huang, H. (2021). Enrichment of *Burkholderia* in the
594 Rhizosphere by Autotoxic Ginsenosides to Alleviate Negative Plant-Soil Feedback.
595 *Microbiology Spectrum*, 9, e0140021. doi: 10.1128/spectrum.01400-21

596 Luo, Q., Hiessl, S., Steinbüchel, A. (2014). Functional diversity of *Nocardia* in metabolism.
597 *Environmental Microbiology*, 16, 29–48. doi: 10.1111/1462-2920.12221

598 Magoč, T., Salzberg, S.L. (2011). FLASH: fast length adjustment of short reads to improve genome
599 assemblies. *Bioinformatics* , 27, 2957–2963. doi: 10.1093/bioinformatics/btr507

600 Miquel Guennoc, C., Rose, C., Labbé, J., Deveau, A. (2018). Bacterial biofilm formation on the
601 hyphae of ectomycorrhizal fungi: a widespread ability under controls? *FEMS Microbiology*
602 *Ecology*, 94, 10.1093/femsec/fiy093. doi: 10.1093/femsec/fiy093

603 Moeller, H.V., Peay, K.G. (2016). Competition-function tradeoffs in ectomycorrhizal fungi. *PeerJ*, 4,
604 e2270. doi: 10.7717/peerj.2270

605 Nehls, U., Göhringer, F., Wittulsky, S., Dietz, S. (2010). Fungal carbohydrate support in the
606 ectomycorrhizal symbiosis: a review. *Plant Biology*, 12, 292–301. doi: 10.1111/j.1438-
607 8677.2009.00312.x

608 Nehls, U., Plassard, C. (2018). Nitrogen and phosphate metabolism in ectomycorrhizas. *New*
609 *Phytologist*, 220, 1047–1058. doi: 10.1111/nph.15257

610 Nguyen, N.H., Bruns, T.D. (2015). The Microbiome of *Pinus muricata* Ectomycorrhizae:
611 Community Assemblages, Fungal Species Effects, and *Burkholderia* as Important Bacteria in
612 Multipartnered Symbioses. *Microbial Ecology*, 69, 914–921. doi: 10.1007/s00248-015-0574-
613 y

614 Nishida, M., Mine, Y., Nonoyama, S., Kojo, H. (1977). Nocardicin A, a new monocyclic beta-lactam
615 antibiotic III. In vitro evaluation. *The Journal of Antibiotics*, 30, 917–925. doi:
616 10.7164/antibiotics.30.917

617 Ogawa, M. (1977). Microbial ecology of 'Shiro' in *Tricholoma matsutake* (S. Ito & Imai) Sing. and
618 its allied species. V. *Tricholoma matsutake* in *Tsuga sieboldii* forests. *Transactions of the*
619 *Mycological Society of Japan*, 18, 34-46.

620 Oh, S.Y., Fong, J.J., Park, M.S., Lim, Y.W. (2016). Distinctive Feature of Microbial Communities
621 and Bacterial Functional Profiles in *Tricholoma matsutake* Dominant Soil. *PLOS ONE*, 11,
622 e0168573–e0168573. doi: 10.1371/journal.pone.0168573

623 Olanrewaju, O.S., Babalola, O.O. (2019). *Streptomyces*: implications and interactions in plant growth
624 promotion. *Applied Microbiology and Biotechnology*, 103, 1179–1188. doi: 10.1007/s00253-
625 018-09577-y

626 Ota, Y., Yamanaka, T., Murata, H., Neda, H., Ohta, A., Kawai, M., et al. (2012). Phylogenetic
627 relationship and species delimitation of*matsutake*and allied species based on multilocus
628 phylogeny and haplotype analyses. *Mycologia*, 104, 1369–1380. doi: 10.3852/12-068

629 Poole, E.J., Bending, G.D., Whipps, J.M., Read, D.J. (2001). Bacteria associated with *Pinus*
630 *sylvestris-Lactarius rufus* ectomycorrhizas and their effects on mycorrhiza formation in vitro.
631 *New Phytologist*, 151, 743–751. doi: 10.1046/j.0028-646x.2001.00219.x

632 Quan, X.L., Fu, W.J., Wu, J.R. (2005). Experiments on the Best Selected Part of Tissue Separation of
633 *Tricholoma bakamatsutake*. *Edible Fungi of China*, 5, 19-20.

634 Quan, X.L., Wang, H.J., Shi, T.Y., Zhang, M.S. (2007). Comparison of the nutritional composition of
635 the seeds of *Tricholoma matsutake* and *Tricholoma bakamatsutake*. *Edible Fungi*, 2, 54–55.

636 Read, D.J., Perez-Moreno, J. (2003). Mycorrhizas and nutrient cycling in ecosystems – a journey
637 towards relevance? *New Phytologist*, 157, 475–492. doi: 10.1046/j.1469-8137.2003.00704.x

638 Requena, N., Jimenez, I., Toro, M., Barea, J.M. (1997). Interactions between plant-growth-promoting
639 rhizobacteria (PGPR), arbuscular mycorrhizal fungi and *Rhizobium* spp. in the rhizosphere of
640 *Anthyllis cytisoides*, a model legume for revegetation in mediterranean semi-arid ecosystems.
641 *New Phytologist*, 136, 667–677. doi: 10.1046/j.1469-8137.1997.00786.x

642 Riedlinger, J., Schrey, S.D., Tarkka, M.T., Hampp, R., Kapur, M., Fiedler, H.P. (2006). Auxofuran, a
643 Novel Metabolite That Stimulates the Growth of Fly Agaric, Is Produced by the Mycorrhiza
644 Helper Bacterium *Streptomyces* Strain AcH 505. Applied and Environmental Microbiology
645 72, 3550–3557. doi: 10.1128/aem.72.5.3550-3557.2006

646 Rigamonte, T.A., Pylro, V.S., Duarte, G.F. (2010). The role of mycorrhization helper bacteria in the
647 establishment and action of ectomycorrhizae associations. *Brazilian journal of microbiology :*
648 *[publication of the Brazilian Society for Microbiology]*, 41, 832–840. doi: 10.1590/S1517-
649 83822010000400002

650 Samuels, L., Kunst, L., Jetter, R. (2008). Sealing Plant Surfaces: Cuticular Wax Formation by
651 Epidermal Cells. *Annual Review of Plant Biology*, 59, 683–707. doi:
652 10.1146/annurev.arplant.59.103006.093219

653 Schloss, P.D., Westcott, S.L., Ryabin, T., Hall, J.R., Hartmann, M., Hollister, E.B., et al. (2009).
654 Introducing mothur: Open-Source, Platform-Independent, Community-Supported Software
655 for Describing and Comparing Microbial Communities. *Applied and Environmental*
656 *Microbiology*, 75, 7537–7541. doi: 10.1128/aem.01541-09

657 Shokralla, S., Spall, J.L., Gibson, J.F., Hajibabaei, M. (2012). Next-generation sequencing
658 technologies for environmental DNA research. *Molecular Ecology*, 21, 1794–1805. doi:
659 10.1111/j.1365-294x.2012.05538.x

Singha, L.P., Pandey, P. (2021). Rhizosphere assisted bioengineering approaches for the mitigation of petroleum hydrocarbons contamination in soil.*Critical reviews in biotechnology*, 41, 749–766. doi: 10.1080/07388551.2021.1888066

Song, Y.Y., Simard, S.W., Carroll, A., Mohn, W.W., Zeng, R.S. (2015). Defoliation of interior Douglas-fir elicits carbon transfer and stress signalling to ponderosa pine neighbors through ectomycorrhizal networks. *Scientific Reports*, 5, 8495. doi: 10.1038/srep08495

Stackebrandt, E., Goebel, B.M. (1994). Taxonomic Note: A Place for DNA-DNA Reassociation and 16S rRNA Sequence Analysis in the Present Species Definition in Bacteriology. *International Journal of Systematic and Evolutionary Microbiology*, 44, 846–849. doi: 10.1099/00207713-44-4-846

Tedersoo, L., Bahram, M., Zobel, M. (2020). How mycorrhizal associations drive plant population and community biology. *Science*, 367, eaba1223. doi: 10.1126/science.aba1223

Terashima, Y. (1990). Carbon and nitrogen utilization and acid production by mycelia of the ectomycorrhizal fungus *Tricholoma bakamatsutake* in vitro. *Mycoscience*, 40, 51–56. doi: 10.1007/bf02465673

Terashima, Y. (1994). Change in medium components and colony morphology due to mycelial growth of ectomycorrhizal fungus *Tricholoma bakamatsutake*. *Mycoscience*, 35, 153–159. doi: 10.1007/bf02318493

Timonen, S., Hurek, T. (2006). Characterization of culturable bacterial populations associating with *Pinus sylvestris–Suillus bovinus* mycorrhizospheres. Canadian Journal of *Microbiology*, 52, 769–778. doi: 10.1139/w06-016

Vaario, L.M., Fritze, H., Spetz, P., Heinonsalo, J., Hanajík, P., Pennanen, T. (2011). *Tricholoma matsutake* Dominates Diverse Microbial Communities in Different Forest Soils. *Applied and Environmental Microbiology*, 77, 8523–8531. doi: 10.1128/aem.05839-11

van Scholl, L., Hoffland, E., van Breemen, N. (2006). Organic anion exudation by ectomycorrhizal fungi and *Pinus sylvestris* in response to nutrient deficiencies. *New Phytologist*, 170, 153–163. doi: 10.1111/j.1469-8137.2006.01649.x

Verma, V.C., Singh, S.K., Prakash, S. (2011). Bio-control and plant growth promotion potential of siderophore producing endophytic *Streptomyces* from *Azadirachta indica* A. Juss. *Journal of Basic Microbiology*, 51, 550–556. doi: 10.1002/jobm.201000155

Wall, L.G. (2000). The Actinorhizal Symbiosis. *Journal of Plant Growth Regulation*, 19, 167–182. doi: 10.1007/s003440000027

Wang, J.L., Liu, K.L., Zhao, X.Q., Gao, G.F., Wu, Y., Shen, R.F. 2022. Microbial keystone taxa drive crop productivity through shifting aboveground-belowground mineral element flows. *Science of The Total Environment*, 811, 152342–152342. doi: 10.1016/j.scitotenv.2021.152342

Wang, Q., Garrity, G.M., Tiedje, J.M., Cole, J.R. (2007). Naive Bayesian Classifier for Rapid Assignment of rRNA Sequences into the New Bacterial Taxonomy. *Applied and Environmental Microbiology*, 73, 5261–5267. doi: 10.1128/aem.00062-07

Wu, Q.S., Liu, J.S., Quan, X.L. (2009). Experiment on optimizing the culture medium of *Tricholoma bakamatsutake* parent species in Changbai Mountain area. *Edible Fungi*, 2, 32–33.

Xu, Y. (2021). Soil Microbial Diversity in the Habitat of *Tricholoma matsutake* in Northeast China. [Dissertation], [Jilin]: Jilin Agricultural University

Yamanaka, T. (2003). The effect of pH on the growth of saprotrophic and ectomycorrhizal ammonia fungi in vitro. *Mycologia*, 95, 584–589. doi: 10.1080/15572536.2004.11833062

Yamanaka, T., Konno, M., Kawai, M., Ota, Y., Nakamura, N., Ohta, A. (2019). Improved chlamydospore formation in *Tricholoma bakamatsutake* with addition of amino acids in vitro. *Mycoscience*, 60, 319–322. doi: 10.1016/j.myc.2019.06.003

Yang, C., Zeng, Z., Zhang, H., Gao, D., Wang, Y., He, G., et al. (2022). Distribution of sediment microbial communities and their relationship with surrounding environmental factors in a typical rural river, Southwest China. *Environmental Science and Pollution Research*, 29, 84206–84225. doi: 10.1007/s11356-022-21627-7

Yang, M., Qi, Y., Liu, J., Wu, Z., Gao, P., Chen, Z. (2022). Dynamic changes in the endophytic bacterial community during maturation of *Amorphophallus muelleri* seeds. *Frontiers in Microbiology*, 13, 996854. doi: 10.3389/fmicb.2022.996854

Yeats, T.H., Rose, J.K. (2013). The Formation and Function of Plant Cuticles. *Plant Physiology*, 163, 5–20. doi: 10.1104/pp.113.222737

Ye, L., Fu, Y., Li, Q., Wang, Q.F., Zhang, B., Zou, J. (2018). Bacterial community structure of *Tricholoma matsutake* stipe soil by high-throughput sequencing. *Chinese Journal of Applied and Environmental Biology*, 24, 583–588. doi: 10.19675/j.cnki.1006-687x.2017.08006

Yu, F., Liang, J.F., Song, J., Wang, S.K., Lu, J.K. (2020). Bacterial Community Selection of *Russula griseocarnosa* Mycosphere Soil. *Frontiers in Microbiology*, 11, 347. doi: 10.3389/fmicb.2020.00347

Yu, J.R., Yuan, H.S. (2023). Research progress on symbiotic interaction and host selection mechanisms of ectomycorrhizal fungi. *Mycosystema*, 42, 86-100. doi: 10.13346/j.mycosystema.220360

Yun, W., Hall, I.R., Evans, L.A. (1997). Ectomycorrhizal fungi with edible fruiting bodies 1.*Tricholoma matsutake* and Related Fungi. *Economic Botany*, 51, 311–327. doi: 10.1007/bf02862101

Zhang, Y., Hu, A., Zhou, J., Zhang, W., Li, P. (2020). Comparison of bacterial communities in soil samples with and without tomato bacterial wilt caused by *Ralstonia solanacearum* species complex. *BMC Microbiology*, 20, 89. doi: 10.1186/s12866-020-01774-y

Zhang, Y.J., Liao, Z.Y., Zhao, B.S. (2020). Glycine betaine: biosynthesis and biological function in halophilic microorganisms. *Acta Microbiologica Sinica*, 60, 1074-1089. doi: 10.13343/j.cnki.wsxb.20190536.

Ziv, C., Zhao, Z., Gao, Y.G., Xia, Y. (2018). Multifunctional Roles of Plant Cuticle During Plant-Pathogen Interactions. *Frontiers in Plant Science*, 9, 1088. doi: 10.3389/fpls.2018.01088

9 Supplementary Material

Supplementary Material

The Supplementary Material for this article can be found online at:

Supplementary Figure 1 | Alpha-diversity of bacterial and fungal communities of the different groups.

Supplementary Figure 2 | Venn diagram of operational taxonomic unit (OTU) numbers of the different groups.

Supplementary Figure 3 | UpSet Venn diagram of fungal OTU number in the different groups. (a) Tb group; (b) CK group. Set Size (top bar) is a count of the number of OTUs in each group itself. Intersection Size (bottom bar) is a count of the number of OTUs for each group after taking the intersection, with the individual dots below indicating OTUs specific to one group and the line between the dots indicating OTUs for the intersection of different groups. OTU, operational taxonomic unit; Tb, *Tricholoma bakamatsutake* shiro soils; CK, *Quercus mongolica* rhizosphere soils.

Supplementary Figure 4 | UpSet Venn diagram of bacterial OTU number in the different groups. (a) Tb group; (b) CK group. Set Size (top bar) is a count of the number of OTUs in each group itself. Intersection Size (bottom bar) is a count of the number of OTUs for each group after taking the intersection, with the individual dots below indicating OTUs specific to one group and the line between the dots indicating OTUs for the intersection of different groups. OTU, operational taxonomic unit; Tb, *Tricholoma bakamatsutake* shiro soils; CK, *Quercus mongolica* rhizosphere soils.

Supplementary Figure 5 | Differences in microbial community structure of the different groups.

Supplementary Figure 5 | Significance analysis of genus-level differences in fungal communities. (a) Kruskal-Wallis H test; (b) Wilcoxon rank-sum test.

Supplementary Figure 7 | Significance analysis of genus-level differences in bacterial communities. (a) Kruskal-Wallis H test; (b) Wilcoxon rank-sum test.

Supplementary Figure 8 | Significance analysis of the differences in the abundance of MHB in different groups. (a) Kruskal-Wallis H test; (b) Wilcoxon rank-sum test. MHB, mycorrhization helper bacteria.

Supplementary Figure 9 | Analysis of the significant differences in the predicted function of PICRUSt2 in fungal communities.

Supplementary Figure 10 | Significant differences in the functional prediction of fungal communities (top 5).

Supplementary Figure 11 | Analysis of significant differences in the predicted function of Phylogenetic Investigation of Communities by Reconstruction of Unobserved States (PICRUSt2) in bacterial communities.

Supplementary Figure 12 | Significance analysis of the variance of BugBase phenotype predictions for bacterial communities.

Supplementary Figure 13 | Functional prediction of FAPROTAX in bacterial communities.

Supplementary Figure 14 | Spearman's analysis of the correlation between bacteria within bacterial communities.

Supplementary Table 1 | Paired samples t-test of significant differences in soil physicochemical properties for two groups.

Supplementary Table 2 | The raw data results from MiSeq for fungal community.

Supplementary Table 3 | The raw data results from MiSeq for bacterial community.

Supplementary Table 4 | Description of the number of enzymes and pathways.

Figures legends

FIGURE 1. | The composition of fungal communities at the genus level in the different groups. (a) Heatmap; (b) Abundance bubble map. Bubble size and color indicate the abundance and classification of the genus, respectively.

FIGURE 2. | The composition of bacterial communities at the genus level in the different groups. (a) Heatmap; (b) Abundance bubble map. Bubble size and color indicate the abundance and classification of the genus, respectively.

FIGURE 3. | CCA/RDA analysis of the relationship in the microbial communities and environmental factors. (a) Fungal communities; (b) Bacterial communities. AP (r2 = 0.5386, P = 0.001), TP (r2 = 0.7456, P = 0.001), TN (r2 = 0.6587, P = 0.001), sand (r2 = 0.318, P = 0.01), and silt (r2 = 0.5227, P = 0.001) were significant factors that influenced fungal community structure. AK (r2 = 0.2546, P = 0.021), AP (r2 = 0.6052, P = 0.001), TK (r2 = 0.203, P = 0.049), TP (r2 = 0.4041, P = 0.001), TN (r2 = 0.4976, P = 0.001), sand (r2 = 0.2562, P = 0.025), and silt (r2 = 0.4882, P = 0.001) were significant factors that influenced bacterial community structure. CCA/RDA, correspondence analysis/ redundancy analysis.

FIGURE 4. | Heatmap of Spearman correlations in the microbial communities and environmental factors. (a) Fungal communities; (b) Bacterial communities.

FIGURE 5. | Pieplot of fungal community composition at the genus level in the *Quercus mongolica* rhizosphere soil (CK) group. (a) ASCK; (b) KDCK; (c) XBCK; (d) XYCK.

FIGURE 6. | Direct or indirect effects in the members of the *Quercus mongolica-Tricholoma bakamatsutake*-associated bacteria symbiosis. The soil of the *Q. mongolica* forest provides a soil

environment that contributes to the widespread presence of ECM fungi. However, the composition of the soil affects the colonization of different ECM species, and *T. bakamatsutake* may prefer to colonize environments with high sand and low silt levels owing to good aeration, permeability, and poor water storage; hence, the competition for *T. bakamatsutake* is low in this soil. Once *T. bakamatsutake* colonizes the roots of the oak tree, it receives photosynthetic products from the oak tree through its mycorrhizal roots and transports active soil material to the oak tree. As *T. bakamatsutake* grows, its dominance suppresses other fungi and aggregates its companion bacteria, which are beneficial to its growth and development and that of *Q. mongolica*, whereas *Q. mongolica* and *T. bakamatsutake* provide nutrients to these companion bacteria. ECM, ectomycorrhizal.

10 Data Availability Statement

The datasets presented in this study can be found in online repositories. The name of the repository and accession number can be found below: National Center for Biotechnology Information (NCBI) BioProject, https://www.ncbi.nlm.nih.gov/bioproject/, PRJNA955660.

Figure 1.TIF

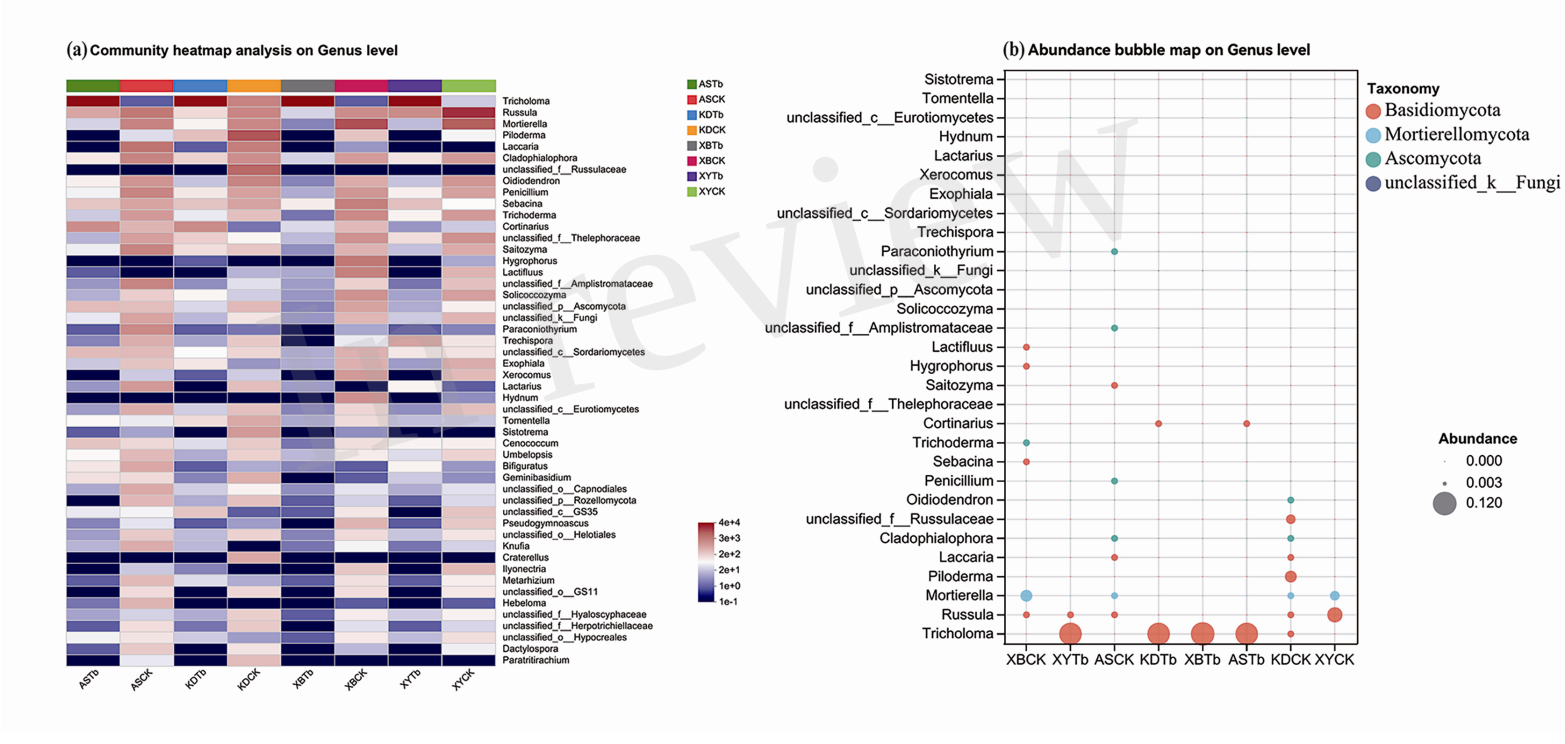
(a) Community heatmap analysis on Genus level
ASTb
ASCK
KDTb
KDCK
XBTb
XBCK
XYTb
XYCK
Tricholoma
Russula
Mortierella
Piloderma
Laccaria
Cladophialophora
unclassified_f__Russulaceae
Oidiodendron
Penicillium
Sebacina
Trichoderma
Cortinarius
unclassified_f__Thelephoraceae
Saitozyma
Hygrophorus
Lactifluus
unclassified_f__Amplistromataceae
Solicoccozyma
unclassified_p__Ascomycota
unclassified_k__Fungi
Paraconiothyrium
Trechispora
unclassified_c__Sordariomycetes
Exophiala
Xerocomus
Lactarius
Hydnum
unclassified_c__Eurotiomycetes
Tomentella
Sistotrema
Cenococcum
Umbelopsis
Bifiguratus
Geminibasidium
unclassified_o__Capnodiales
unclassified_p__Rozellomycota
unclassified_c__GS35
Pseudogymnoascus
unclassified_o__Helotiales
Knufia
Craterellus
Ilyonectria
Metarhizium
unclassified_o__GS11
Hebeloma
unclassified_f__Hyaloscyphaceae
unclassified_f__Herpotrichiellaceae
unclassified_o__Hypocreales
Dactylospora
Paratritirachium
4e+4
3e+3
2e+2
2e+1
1e+0
1e-1
(b) Abundance bubble map on Genus level
Taxonomy
Basidiomycota
Mortierellomycota
Ascomycota
unclassified_k__Fungi
Abundance
0.000
0.003
0.120
XBCK
XYTb
ASCK
KDTb
XBTb
ASTb
KDCK
XYCK

Figure 2.TIF

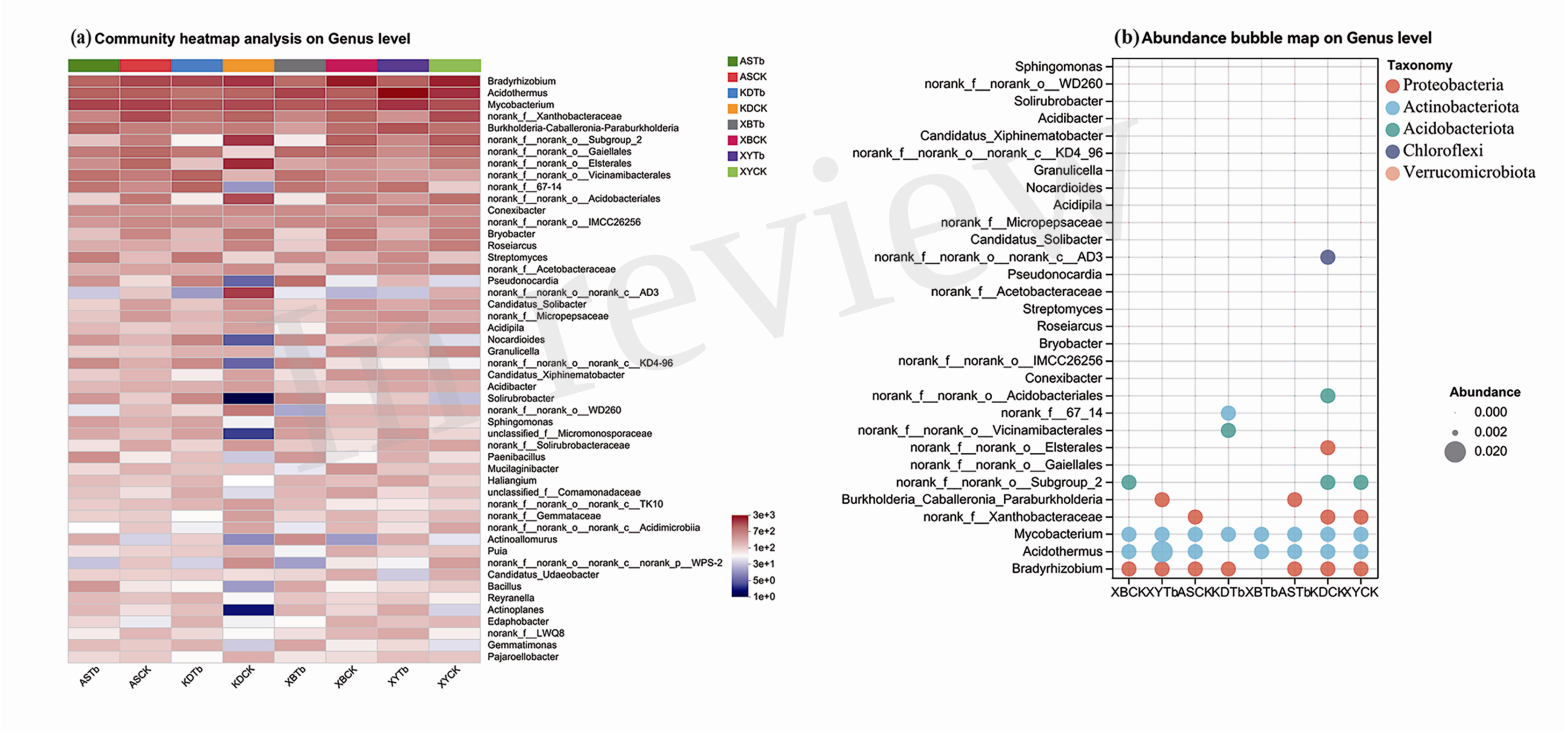
(a) Community heatmap analysis on Genus level
ASTb
ASCK
KDTb
KDCK
XBTb
XBCK
XYTb
XYCK
Bradyrhizobium
Acidothermus
Mycobacterium
norank_f__Xanthobacteraceae
Burkholderia-Caballeronia-Paraburkholderia
norank_f__norank_o__Subgroup_2
norank_f__norank_o__Gaiellales
norank_f__norank_o__Elsterales
norank_f__norank_o__Vicinamibacterales
norank_f__67-14
norank_f__norank_o__Acidobacteriales
Conexibacter
norank_f__norank_o__IMCC26256
Bryobacter
Roseiarcus
Streptomyces
norank_f__Acetobacteraceae
Pseudonocardia
norank_f__norank_o__norank_c__AD3
Candidatus_Solibacter
norank_f__Micropepsaceae
Acidipila
Nocardioides
Granulicella
norank_f__norank_o__norank_c__KD4-96
Candidatus_Xiphinematobacter
Acidibacter
Solirubrobacter
norank_f__norank_o__WD260
Sphingomonas
unclassified_f__Micromonosporaceae
norank_f__Solirubrobacteraceae
Paenibacillus
Mucilaginibacter
Haliangium
unclassified_f__Comamonadaceae
norank_f__norank_o__norank_c__TK10
norank_f__Gemmataceae
norank_f__norank_o__norank_c__Acidimicrobiia
Actinoallomurus
Puia
norank_f__norank_o__norank_c__norank_p__WPS-2
Candidatus_Udaeobacter
Bacillus
Reyranella
Actinoplanes
Edaphobacter
norank_f__LWQ8
Gemmatimonas
Pajaroellobacter
3e+3
7e+2
1e+2
3e+1
5e+0
1e+0
(b) Abundance bubble map on Genus level
Taxonomy
Proteobacteria
Actinobacteriota
Acidobacteriota
Chloroflexi
Verrucomicrobiota
Abundance
0.000
0.002
0.020
XBCK XYTb ASCK KDTb XBTb ASTb KDCK XYCK

Figure 3.TIF

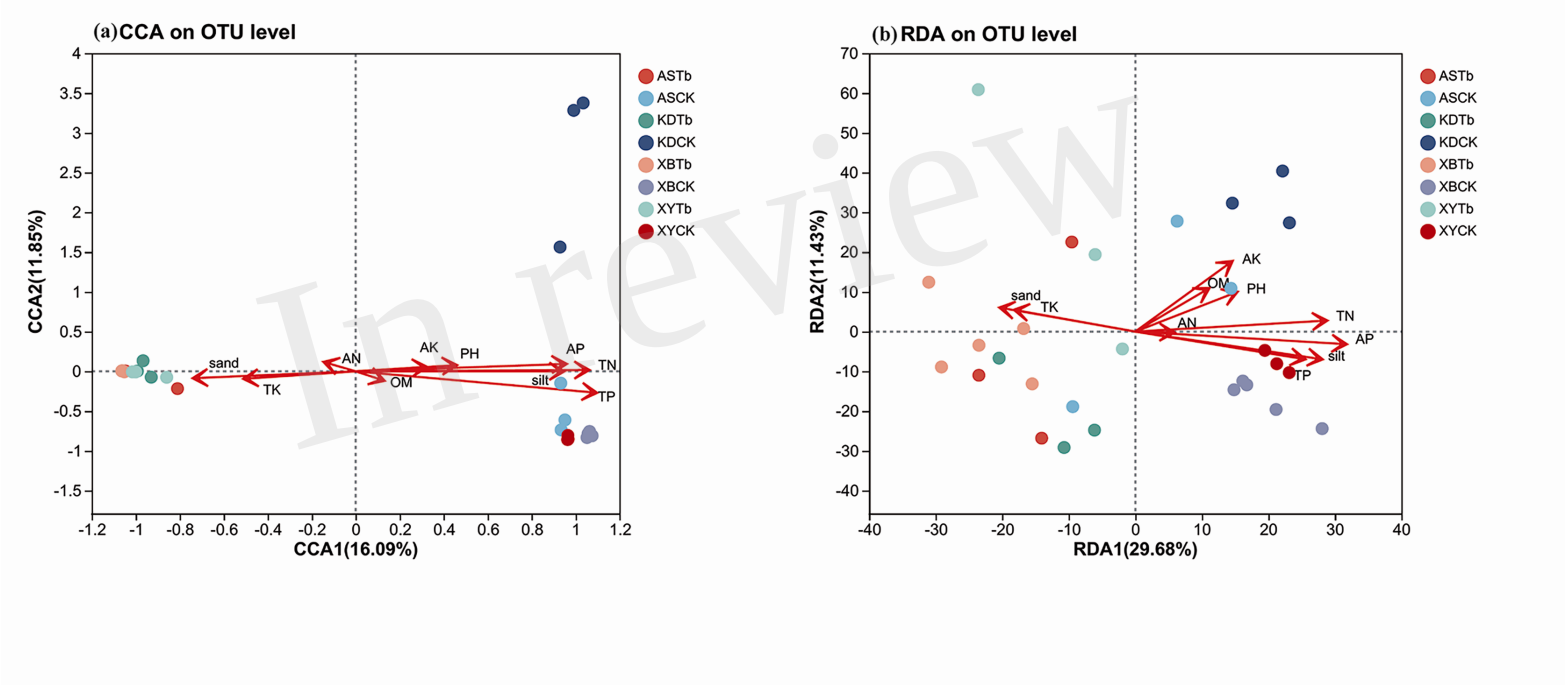

Figure 4.TIF

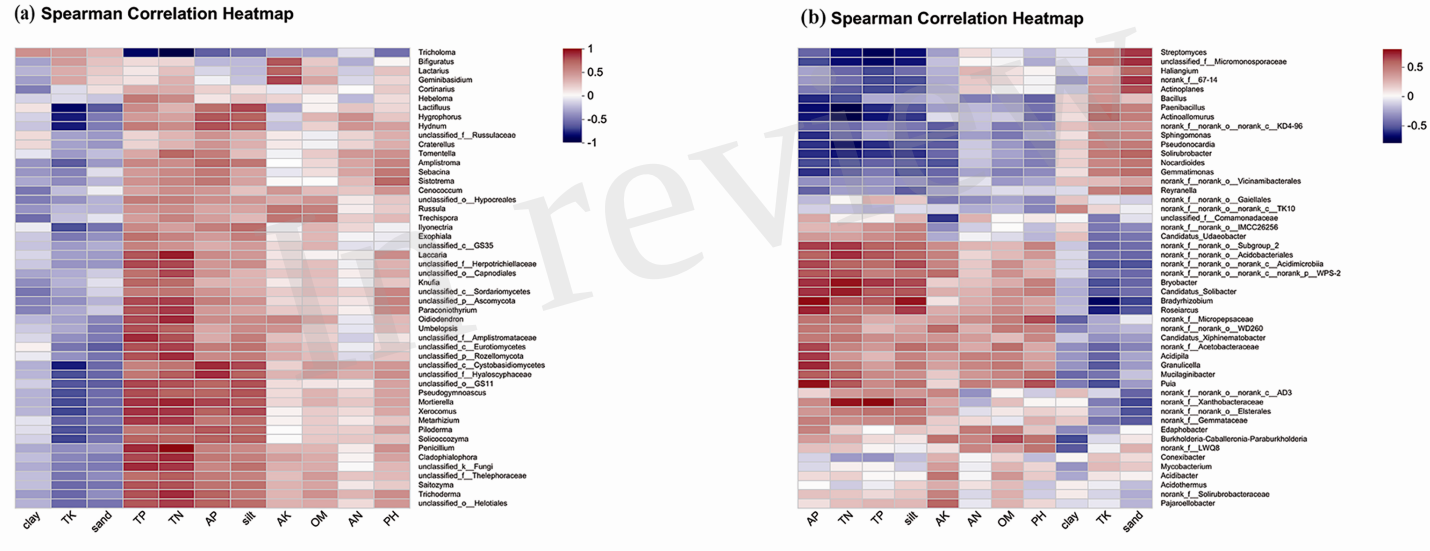
(a) Spearman Correlation Heatmap
Tricholoma
Bifiguratus
Lactarius
Geminibasidium
Cortinarius
Hebeloma
Laciflluus
Hygrophorus
Hydnum
unclassified_f__Russulaceae
Craterellus
Tomentella
Amplistroma
Sebacina
Sistotrema
Cenococcum
unclassified_o__Hypocreales
Russula
Trechispora
Ilyonectria
Exophiala
unclassified_c__GS35
Laccaria
unclassified_f__Herpotrichiellaceae
unclassified_o__Capnodiales
Knufia
unclassified_c__Sordariomycetes
unclassified_p__Ascomycota
Paraconiothyrium
Oidiodendron
Umbelopsis
unclassified_f__Amplistromataceae
unclassified_c__Eurotiomycetes
unclassified_p__Rozellomycota
unclassified_c__Cystobasidiomycetes
unclassified_f__Hyaloscyphaceae
unclassified_o__GS11
Pseudogymnoascus
Mortierella
Xerocomus
Metarhizium
Piloderma
Solicoccozyma
Penicillium
Cladophialophora
unclassified_k__Fungi
unclassified_f__Thelephoraceae
Saitozyma
Trichoderma
unclassified_o__Helotiales
1
0.5
0
-0.5
-1
clay
TK
sand
TP
TN
AP
silt
AK
OM
AN
PH
(b) Spearman Correlation Heatmap
Streptomyces
unclassified_f__Micromonosporaceae
Haliangium
norank_f__67-14
Actinoplanes
Bacillus
Paenibacillus
Actinoallomurus
norank_f__norank_o__norank_c__KD4-96
Sphingomonas
Pseudonocardia
Solirubrobacter
Nocardioides
Gemmatimonas
norank_f__norank_o__Vicinamibacterales
Reyranella
norank_f__norank_o__Gaiellales
norank_f__norank_o__norank_c__TK10
unclassified_f__Comamonadaceae
norank_f__norank_o__IMCC26256
Candidatus_Udaeobacter
norank_f__norank_o__Subgroup_2
norank_f__norank_o__Acidobacteriales
norank_f__norank_o__norank_c__Acidimicrobiia
norank_f__norank_o__norank_c__norank_p__WPS-2
Bryobacter
Candidatus_Solibacter
Bradyrhizobium
Roseiarcus
norank_f__Micropepsaceae
norank_f__norank_o__WD260
Candidatus_Xiphinematobacter
norank_f__Acetobacteraceae
Acidipila
Granulicella
Mucilaginibacter
Puia
norank_f__norank_o__norank_c__AD3
norank_f__Xanthobacteraceae
norank_f__norank_o__Elsterales
norank_f__Gemmataceae
Edaphobacter
Burkholderia-Caballeronia-Paraburkholderia
norank_f__LWO8
Conexibacter
Mycobacterium
Acidibacter
Acidothermus
norank_f__Solirubrobacteraceae
Pajaroellobacter
0.5
0
-0.5
AP
TN
TP
silt
AK
AN
OM
PH
clay
TK
sand

Figure 5.TIF

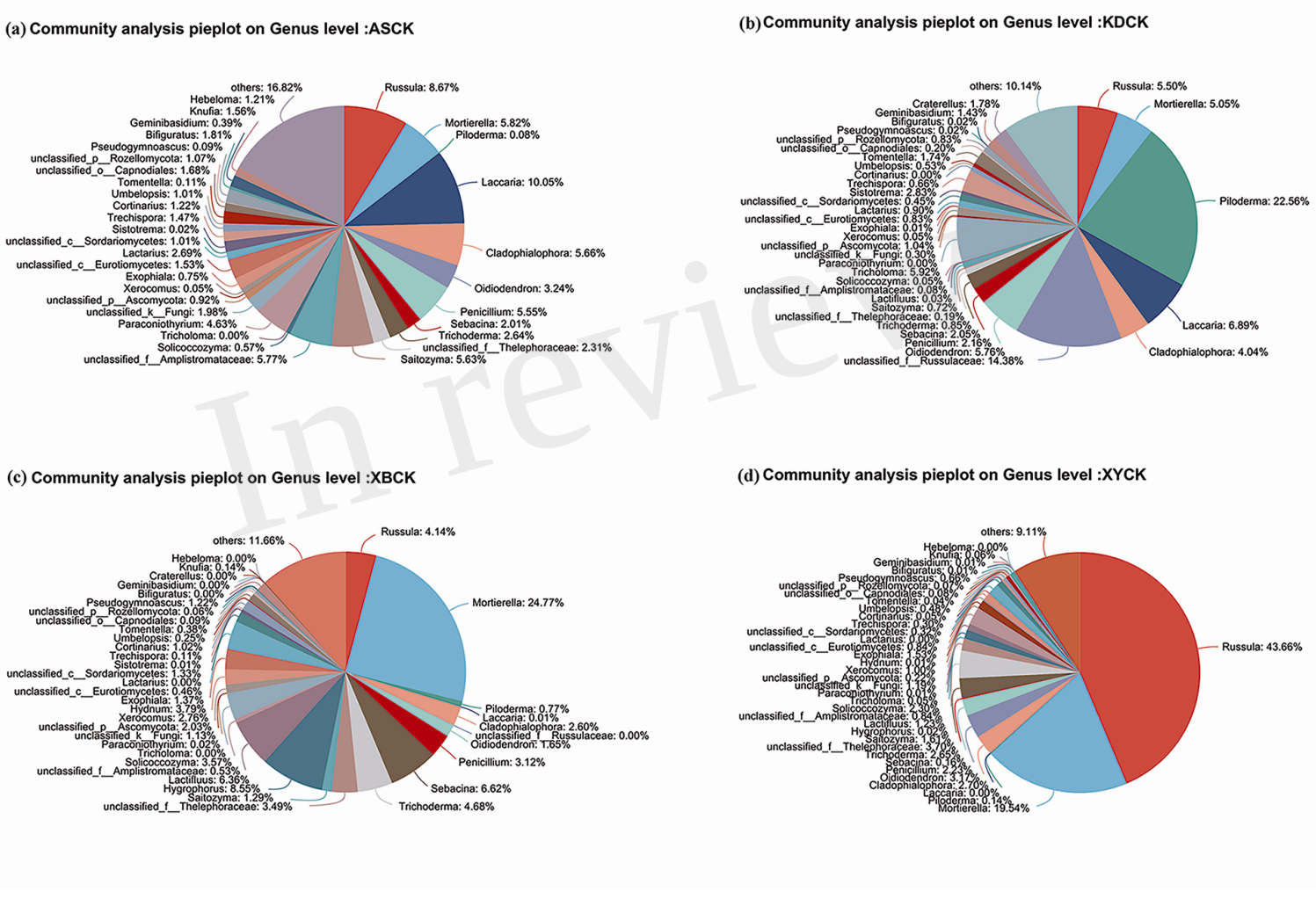

Figure 6.TIF

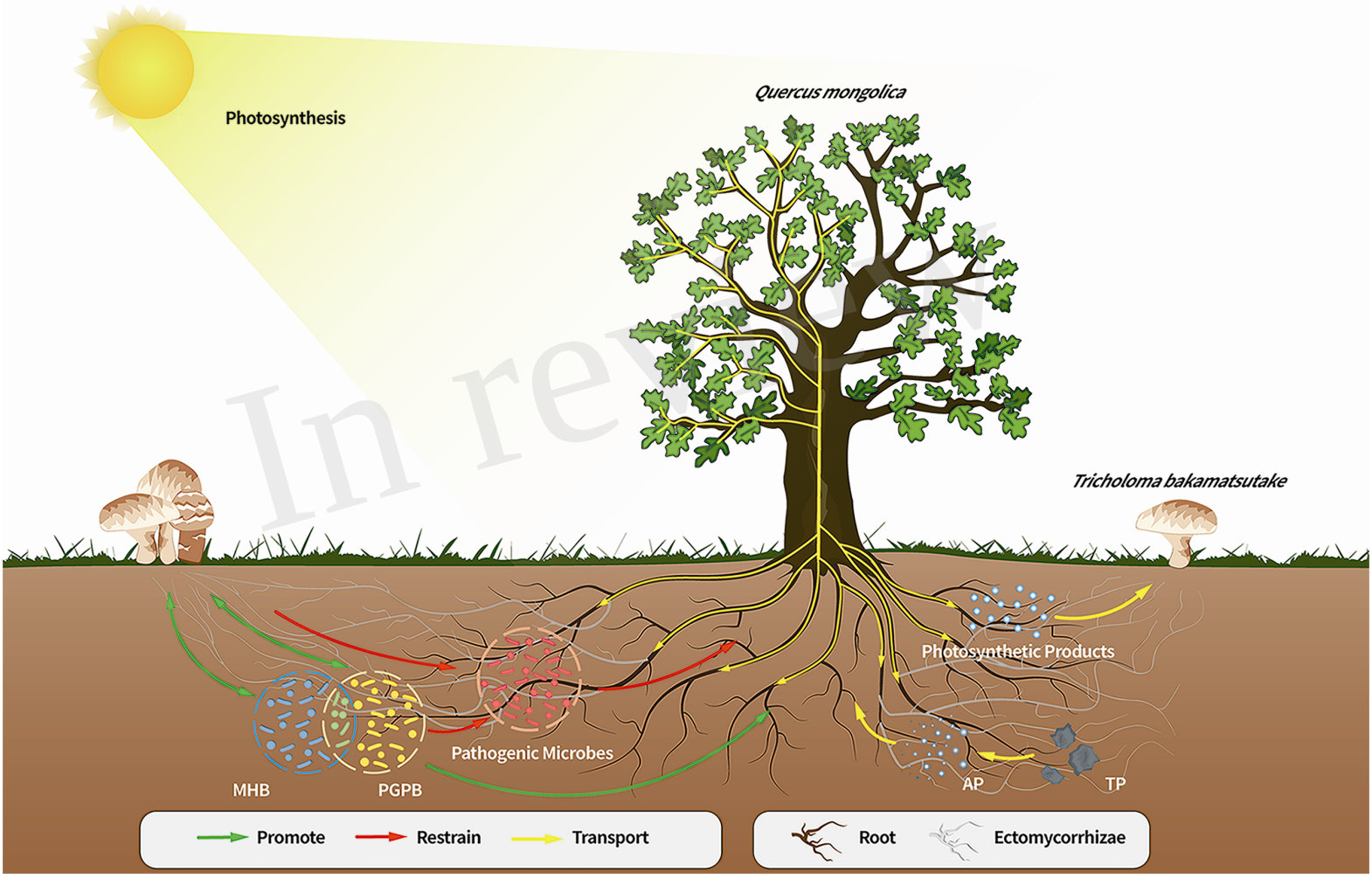
Photosynthesis
Quercus mongolica
Tricholoma bakamatsutake
Photosynthetic Products
Pathogenic Microbes
MHB
PGPB
AP
TP
Promote
Restrain
Transport
Root
Ectomycorrhizae